Spatially-Encoding Hydrogels With DNA to Control Cell Signaling

Namrata Ramani, C. Adrian Figg, Alex J. Anderson, Peter H. Winegar, EunBi Oh, Sasha B. Ebrahimi, Devleena Samanta, and Chad A. Mirkin*

Patterning biomolecules in synthetic hydrogels offers routes to visualize and learn how spatially-encoded cues modulate cell behavior (e.g., proliferation, differentiation, migration, and apoptosis). However, investigating the role of multiple, spatially defined biochemical cues within a single hydrogel matrix remains challenging because of the limited number of orthogonal bioconjugation reactions available for patterning. Herein, a method to pattern multiple oligonucleotide sequences in hydrogels using thiol-yne photochemistry is introduced. Rapid hydrogel photopatterning of hydrogels with micron resolution DNA features (≈1.5 μm) and control over DNA density are achieved over centimeter-scale areas using mask-free digital photolithography. Sequence-specific DNA interactions are then used to reversibly tether biomolecules to patterned regions, demonstrating chemical control over individual patterned domains. Last, localized cell signaling is shown using patterned protein–DNA conjugates to selectively activate cells on patterned areas. Overall, this work introduces a synthetic method to achieve multiplexed micron resolution patterns of biomolecules onto hydrogel scaffolds, providing a platform to study complex spatially-encoded cellular signaling environments.

1. Introduction

A key challenge in predicting cell behavior in vivo is understanding the complexity of cell interactions with the over 300 signaling proteins and proteoglycans in the extracellular matrix (ECM), known as the "matrisome".[1–3] The micro- to nano-scale spatial arrangement of matrisome cues in the ECM drives cellular processes such as migration,[4] endocytosis,[5] differentiation,[6–8]

and angiogenesis.[9] For example, geometric cell-adhesion cues at subcellular length scales (<10 μm) affect focal adhesion complex formation in adherent cells and determine cell morphology (e.g., cytoskeletal organization and shape) and function (e.g., gene expression, survival, and differentiation).[7,10] To elucidate cell behavior in a complex signaling environment, the effect of the spatial arrangement of multiple matrisome cues on cell function is critical to investigate. Cell phenotype has been studied on multiplexed biomolecule surface arrays; however, these substrates are typically stiff materials that fail to capture the biophysical environment of the ECM.[5–7] For instance, human mesenchymal stem cells will differentiate into different lineages depending on the elasticity of a culture matrix.[11] Therefore, there is a need to study cell behavior in an environment that more closely resembles the physical and biochemical environment of the ECM, and tools to control the spatial placement of such cues are becoming increasingly important.[12–17]

Hydrogels offer a synthetically addressable cell culture platform to probe and program cellular behavior due to their hydrophilicity, biocompatibility, and physiologically relevant material properties.[18,19] To mimic the spatial heterogeneity of the ECM, hydrogels can be patterned with biochemical factors (e.g., growth factors,[20] cell-adhesive ligands,[21] and enzyme-cleavable linkers[22]). Click chemistry has enabled the

N. Ramani, C. A. Mirkin
Department of Materials Science and Engineering
Northwestern University
2220 Campus, Drive, Evanston, IL 60208, USA
E-mail: chadnano@northwestern.edu

The ORCID identification number(s) for the author(s) of this article can be found under https://doi.org/10.1002/adma.202301086

N. Ramani, C. A. Figg, A. J. Anderson, P. H. Winegar, E. Oh,
S. B. Ebrahimi, D. Samanta, C. A. Mirkin
International Institute for Nanotechnology
Northwestern University
2190 Campus Drive, Evanston, IL 60208, USA

C. A. Figg, A. J. Anderson, P. H. Winegar, E. Oh, D. Samanta, C. A. Mirkin
Department of Chemistry
Northwestern University
2145 Sheridan Road, Evanston, IL 60208, USA

S. B. Ebrahimi
Department of Chemical and Biological Engineering
Northwestern University
2145 Sheridan Road, Evanston, IL 60208, USA

ADVANCED
SCIENCE NEWS

www.advancedsciencenews.com

ADVANCED
MATERIALS

www.advmat.de

covalent tethering of multiple biomolecules to a hydrogel network through sequential patterning steps without altering the overall network structure or surface topography.[23] In addition, photocleavable groups and dynamic covalent chemistries are used for controlled release of cues, where biomolecules can be cleaved from or reversibly tethered to a hydrogel in the presence of a stimulus (i.e., light).[24–27] While using photocleavable linkers is one method to control biomolecule attachment to or release from a hydrogel, the limitation is the number of available orthogonal photochemistries to address the attachment or detachment of multiple biomolecules.

Oligonucleotides, or short DNA or RNA strands, offer a unique route to directing biomolecular attachment due to their high sequence specificity, ability to bind to specific analytes, and stimuli-responsiveness.[28,29] Biomolecules tagged with DNA can be localized to patterned domains of a complementary DNA sequence through Watson–Crick–Franklin base pairing interactions.[30] In addition, the use of aptamer DNA sequences that selectively bind to molecular targets such as metal ions, small molecules, and proteins, enable the surface tethering of targets without DNA labeling.[31–35] DNA can also undergo strand displacement reactions, offering a dynamic mode for reversibly tethering sequences to a hydrogel.[36] Current photopatterning approaches for DNA hydrogels typically use light-based polymerizations to form bulk DNA hydrogels with specific shapes or subtractive patterning methods. Subtractive patterning methods are where DNA is linked throughout hydrogels via photocleavable *o*-nitrobenzyl linker molecules and removed from specific areas of the gel with UV light to generate patterns.[28,29,37,38] However, these subtractive patterning approaches lack the ability to readily control the attachment of multiple different DNA sequences in adjacent domains. Additive DNA patterns in hydrogels thus far have relied on photomasks, where the demonstrated pattern resolution is ≈400 µm, limiting these gels for studying cues at subcellular length scales (i.e., <10 µm).[34] In addition, with mask-based photolithography, a new photomask needs to be generated for every unique geometric pattern, which makes generating multiplexed high-resolution patterns with arbitrary geometries a challenge.

Herein, we report a strategy to spatially pattern hydrogels with DNA domains at micron-scale resolution. We synthesized hydrogels with pendant alkyne groups as chemical handles for the attachment of thiol-modified oligonucleotides via photomediated thiol-yne chemistry. Oligonucleotides were placed within hydrogels using mask free photolithography ($\lambda = 405$ nm) to create complex patterns on biologically relevant length scales (≈1.5 µm) over centimeter-scale areas. Importantly, this approach enabled patterns with controlled feature size, geometry, and DNA density. Iterative patterning allowed for the patterning of multiple distinct DNA strands, such that the DNA sequence in each domain could dictate the binding properties to complementary oligonucleotides and biomolecular signals of interest. Significantly, we observed that cells located on patterns of signaling proteins can be selectively activated. Taken together, this work introduces a new modular material for interrogating the role of multiplexed biomolecule patterns on cell behavior, with implications in single-cell analysis, developmental biology, and tissue engineering.

2. Results and Discussion

2.1. Hydrogel Synthesis and Photopatterning

Additive photopatterning approaches enable the building of complex synthetic signaling environments from the bottom up. Our goal was to create an additive DNA patterning method where we could discretely control biochemical cues on the single micron length scale. To covalently tether the DNA to the hydrogel network with light, a TERA-Fab E-series photolithography instrument was used. This tool contains a digital micromirror device (DMD), which is an array of 1024 × 768 individually addressable mirrors, coupled with an LED light source (405 nm, 2.8 W) to produce arbitrary light patterns and contains a software-controlled piezoelectric stage which controls *xyz* movement with 1 nm precision. This strategy allows for the parallel printing of multiple features across centimeter-scale areas, patterning of gradient features, and serial printing for multiplexed patterning. Chain-growth, polyethylene glycol (PEG) diacrylate hydrogels were used as synthetic matrix materials because they are non-fouling and tunable according to the reaction conditions (e.g., stiffness can be modulated with monomer to crosslinker ratios).[22,39] To introduce a chemical handle for DNA functionalization, co-monomers with alkyne side chains were incorporated during the hydrogel synthesis (**Figure 1**A). These alkynes are inert to the radical polymerization conditions during hydrogel formation but will react with thiol-modified DNA through thiol-yne click chemistry following hydrogel formation.[25,40–42] Thiol-yne reactions are advantageous because they are biocompatible, high yielding, rapid, have minimal side reactions, and can be initiated with light. To synthesize hydrogels containing alkynes, 2.5 wt% polyethylene glycol diacrylate (PEGDA) and 7.5 wt% polyethylene glycol monoacrylate (PEGMA) system were copolymerized with 1 wt% propargyl acrylate (PA). FTIR analysis confirmed alkyne incorporation in the fully formed hydrogel, where a diagnostic band for $-C\equiv C-$ stretching was observed at 2130 cm^{-1} (Figure S2, Supporting Information). To verify that single stranded DNA (ssDNA) could diffuse through the matrix to react within the network, the mesh size of the hydrogels was calculated to be 10 ± 1 nm (Equation (S1), Supporting Information) using the measured equilibrium swelling ratio of the gels. As a 20 nucleotide (nt) ssDNA molecule is ≈4 nm in size,[43] this mesh size will allow for DNA diffusion through the bulk of the hydrogel.

First, we investigated how DNA functionalization changes according to pattern feature size, irradiation time, and light intensity. Lithium phenyl-2,4,6 trimethylbenzoylphosphinate (LAP) was selected as a photoinitiator due to its water solubility, rapid rate of photolysis, and cytocompatibility.[44] Gels were swollen in a solution with 20 µM of thiol-modified T_{20} oligonucleotide labeled with a Cyanine 3.5 fluorophore (Strand A; Table S1, Supporting Information) and different equivalents of LAP and patterned with the TERA-Fab E-series (Figure 1B). Irradiated gels were washed with 1× PBS overnight to remove unreacted DNA and imaged using fluorescence wide field microscopy and confocal microscopy. At 0.5 equivalents or lower initiator concentrations, DNA functionalization occurred solely in the areas of the hydrogel exposed to light, and DNA functionalization increased with LAP concentration (Figure S6, Supporting Information). Inverse features were observed with high intensities and
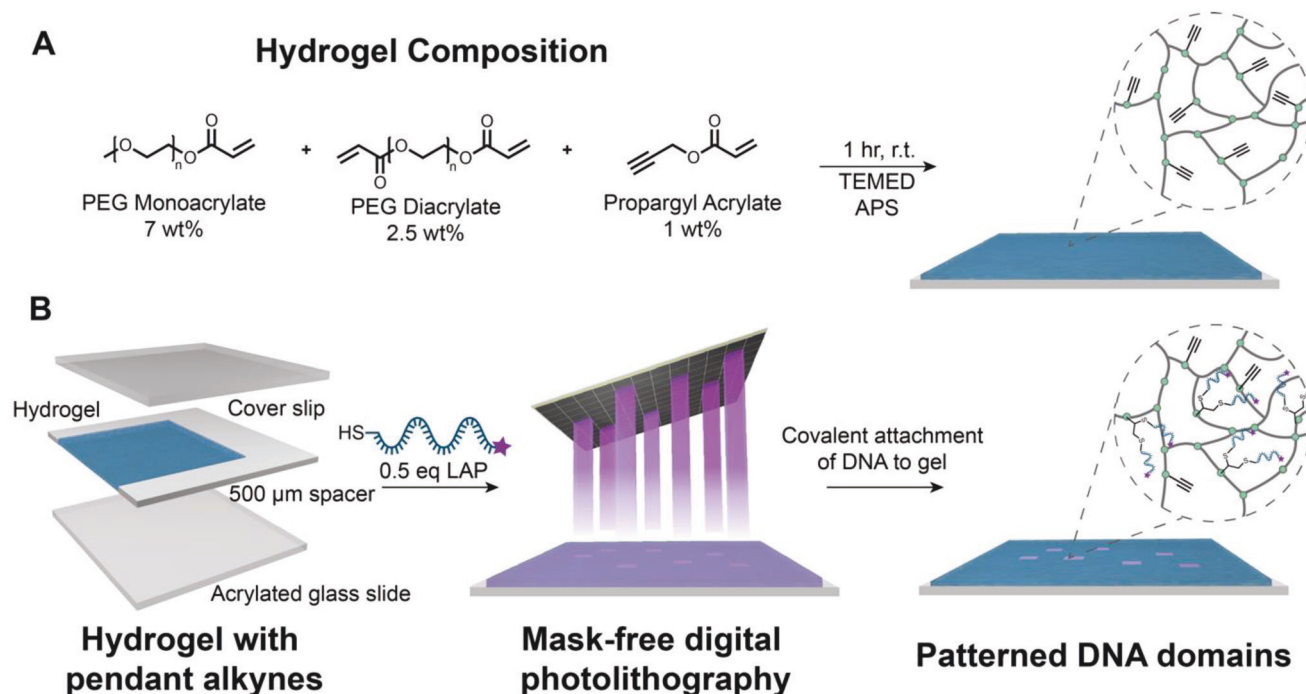
Figure 1. A) Synthesis of PEG hydrogels with pendant alkyne groups. B) Workflow for photopatterning hydrogels with DNA. Hydrogel thin films are synthesized on acrylate functionalized glass slides. Thiol-terminated DNA is introduced and allowed to diffuse through the gel network. A Tera-FAB E-Series instrument is used to irradiate gels, enabling covalent attachment of DNA to the network. After removal of excess DNA through washing, the DNA is localized to patterned areas.

irradiation times when the initiator concentration was higher than 0.5 equivalents relative to thiol, where DNA was solely functionalized outside of the irradiated area (Figure S9, Supporting Information). This dependence on photoinitiator concentrations was likely due to the concentration of radicals in the irradiated areas. At high initiator concentrations, there will be high radical concentrations in the irradiated portions of the gels, leading to premature radical-radical coupling termination events instead of initiation and propagation of the thiol-yne reaction. Meanwhile, the small number of radicals that diffuse outside of irradiated areas (where the concentration of radicals is lower) will initiate the thiol-yne reaction, resulting in the observed inverse patterns. If the concentration of initiator is low enough to avoid pre-mature termination (i.e., <0.5 equivalents relative to thiol), the thiol-yne reaction proceeds in the patterned area before significant unwanted termination.

For probing cell–ECM interactions for individual cells, control over DNA density and spatial attachment at subcellular length scales (<10 µm) needs to be realized. To analyze the resolution of patterned features of varying sizes, line profiles were taken from confocal micrographs imaged at the surface of the hydrogels patterned with varying light exposure areas (**Figure 2**A; Figure S10, Supporting Information). Spatial resolution was determined by calculating the average full width at half maximum of the intensity peaks from line profiles (Figure S10, Supporting Information). The smallest high-fidelity features observed with DMD photopatterning were 1.36 ± 0.33 µm in edge length. Notably, this feature size is the smallest DNA pattern within hydrogels reported to date. Patterns were found to have sharp interfaces

between irradiated and non-irradiated portions, independent of feature size. Importantly, this indicates that radical diffusion outside the patterns was limited when photoinitiator concentrations were at or below 0.5 equivalents, and that DMD photopatterning results in discrete patterns with micron-scale resolution. Next, the effect of irradiation time and light intensity on DNA attachment were investigated to study how local DNA concentration could be controlled. Confocal analysis was combined with DNA loading measurements to quantify the amount of DNA in each pattern. To perform the loading measurements, hydrogels were degraded using 0.1 M NaOH and the average DNA concentration over the patterned area was determined from the Cy3.5 fluorescence (Figure 2B–E). The efficiency of the LAP photolysis and thiol-yne reaction yields rapid DNA functionalization (within 10 s of irradiation), which minimizes gel dehydration during the patterning process. Measured DNA concentration values followed similar trends as confocal image analysis of patterned features (Figure S8, Supporting Information). Understanding that light intensity and irradiation time can be used to control DNA functionalization, continuous linear DNA gradients were patterned by moving the hydrogel along the xy plane at a constant rate of 2 µm s^{-1} during irradiation (Figure 2F). Overall, the key parameters that dictate successful patterning of DNA using this method are: 1) the successful incorporation of alkyne functional groups within the hydrogel, 2) diffusion of thiol-terminated DNA sequences through the gel network, 3) using less than 0.5 equivalents of LAP photoinitiator to thiol to prevent inverse feature formation, and 4) removal of unreacted DNA from the gel through washing.
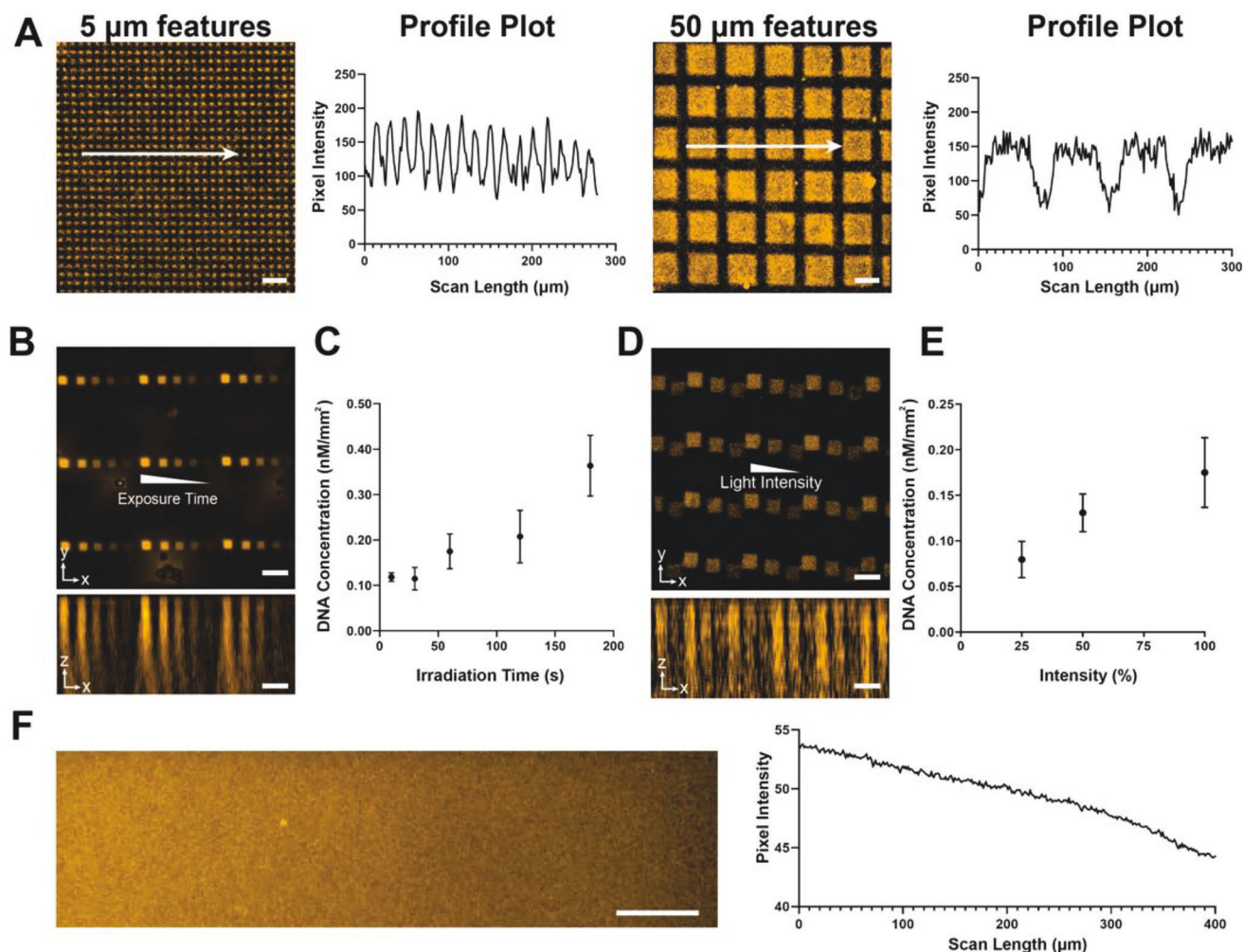
Figure 2. A) Confocal micrographs of hydrogels patterned with 5 and 50 µm features, along with associated profile plots. B) Confocal *z*-stack of hydrogel patterned with features of varying exposure time (from left to right: 180, 120, 60, 30, and 10 s). C) Hydrogel loading measurements of gels patterned with varying exposure time. The data are represented as the mean DNA concentration ± S.D. (*n* = 3). D) Confocal *z*-stack of hydrogel patterned with features of varying LED intensity (from left to right: 100%, 50%, and 25%). E) DNA loading measurements of gels patterned with varying LED intensity (*n* = 3). The data are represented as the mean DNA concentration ± S.D. (*n* = 3). F) Confocal micrograph and associated profile plot of gradient hydrogel. Gradient generated by moving light source at constant rate across surface, creating a gradient of exposure time across the surface. Scale bars = 50 µm.

After evaluating the surface functionalization of the hydrogels with DNA, we sought to characterize how patterning conditions affected the *z*-depth of the patterned features. Confocal *z*-stacks of patterned hydrogels were taken to determine the depth of functionalization. The functionalization depth was measured to be ≈250 µm for all gels patterned with 0.5 equivalents of photoinitiator, independent of feature size, light intensity, and irradiation time. Moreover, the confocal *z*-stacks showed uniform fluorescence through the bulk of the feature, with fluorescence intensity dependent on irradiation time or intensity (Figure S11, Supporting Information). These data suggest that the depth of the feature is determined by the attenuation of the light within the hydrogel, and the lack of gradient suggests that thiyl radicals do not readily diffuse out or covalently attach to the gel network outside of the irradiated region.

2.2. Using DNA Sequence to Direct Chemical Functionality

The additive photopatterning approach allows for patterning of multiple sequences in registry, where the sequence identity of DNA provides specific and orthogonal interactions in each patterned domain. To test the modularity of photopatterning PEG hydrogels using DMD, patterning of different DNA designed sequences was investigated using iterative steps. Through stage alignment of the Tera-FAB E-series using *xy* coordinate markings, micron-scale DNA domains of T_{20} labeled with three different fluorophores (Strand A, Strand B, and Strand C) were patterned sequentially next to each other (**Figure 3**A). First, Strand A was patterned, and the hydrogels were washed with 1× PBS. After sufficient removal of unreacted Strand A, the gels were swollen with a solution of Strand B and photoinitiator and

**ADVANCED
SCIENCE NEWS**

www.advancedsciencenews.com
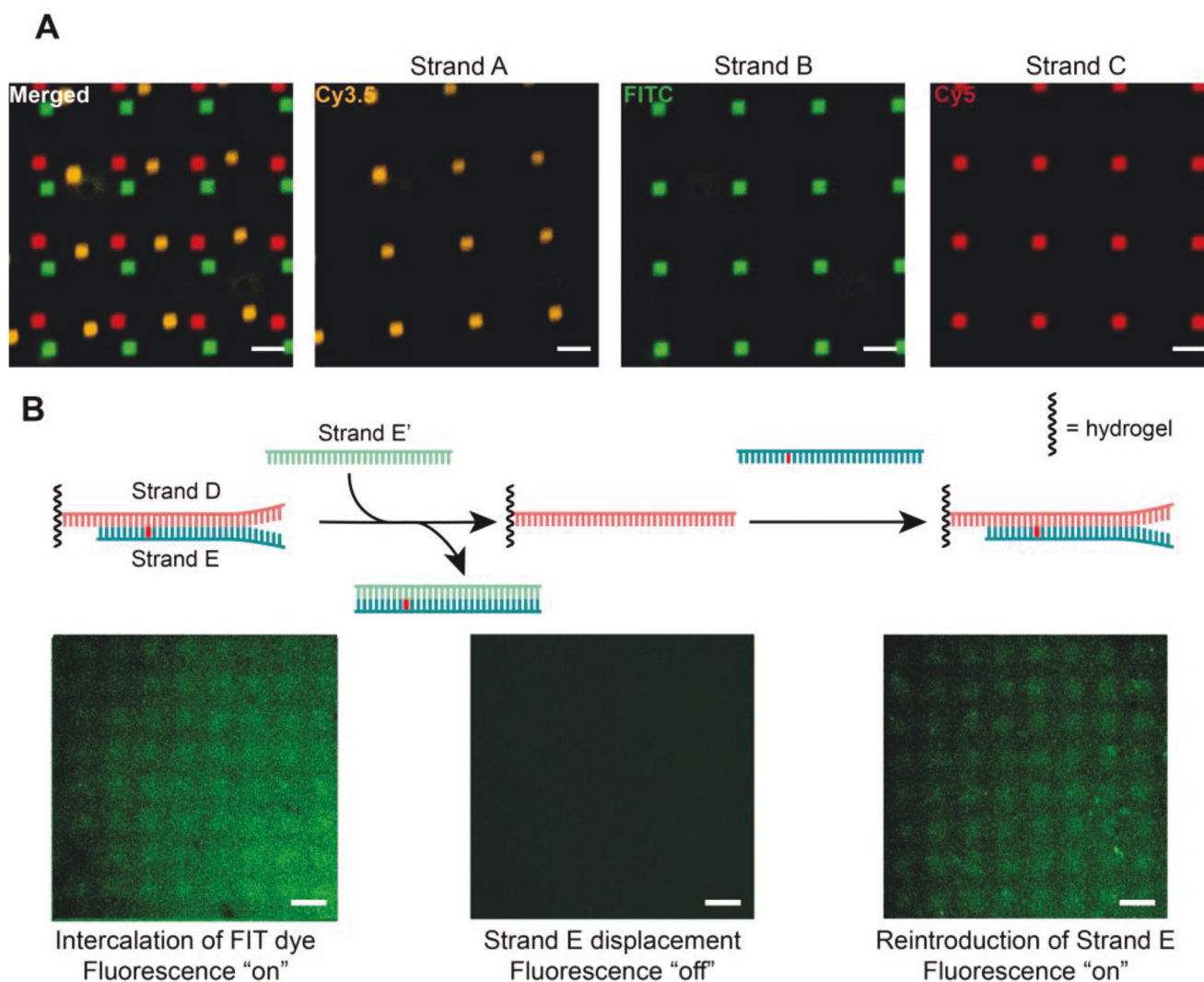
**ADVANCED
MATERIALS**

www.advmat.de

Figure 3. A) Iterative patterning of Strand A, Strand B, and Strand C in a single hydrogel. Confocal micrographs show functionalization of three distinct sequences in 20 µm square patterns with pattern registry between features. B) Strand displacement reaction shows reversible tethering of hybridized sequence. First Strand D was patterned in the gel. Strand E, containing a forced intercalation thiazole orange dye was introduced, and fluorescence turn on was observed in confocal micrographs of the patterns (left). When complementary Strand E' was introduced, Strand E was displaced from the gel, and fluorescence turn off was observed (Middle). Fluorescence was restored in patterns when Strand E was reintroduced (Right). Scale bars = 50 µm.

patterned again. This process was repeated a third time to pattern Strand C. In addition, we patterned the three sequences in overlapping areas (Figures S13 and S14, Supporting Information) and observed that domains could be patterned containing multiple sequences. To test if sequence-specific binding was feasible inside the hydrogel, Strand A and another 20 nt oligonucleotide sequence (Strand H), both labeled with Cy3.5, were patterned in a hydrogel sequentially (Figure S14, Supporting Information). Next, Cy5-labeled Strand H', a complementary oligonucleotide sequence to Strand H, was introduced. Confocal micrographs show that fluorescence in the Cy5 channel was only localized to the patterns of Strand H, demonstrating that the specific Strand H-Strand H' DNA interactions are what tethers Strand H' to the gel. Extending this iterative patterning approach could lead to highly encoded hydrogels as this method is generalizable to any oligonucleotide sequence with a thiol functional group. For

example, through the design of 20 nt DNA anchor sequences, 4^{20} ($\approx 10^{12}$), unique interactions can be programmed in a hydrogel, using one DNA attachment chemistry. The number of possible sequences further grows when we consider anchor sequences of different lengths.

Beyond the static spatial arrangement of cues in the ECM, the dynamics of cue release from the ECM on the time scales of seconds to days can dictate cell phenotype and disease progression.[1] DNA strand displacement offers dynamic control, where a prehybridized DNA sequence can be displaced from a DNA duplex upon introduction of a third strand with increased binding affinity. Here, a complementary sequence (Strand E) to an anchored DNA sequence (Strand D) was designed, containing an 8 base mismatch region. We predicted that in the presence of Strand E', which is fully complementary to Strand E, removal of Strand E from the hydrogel matrix would be
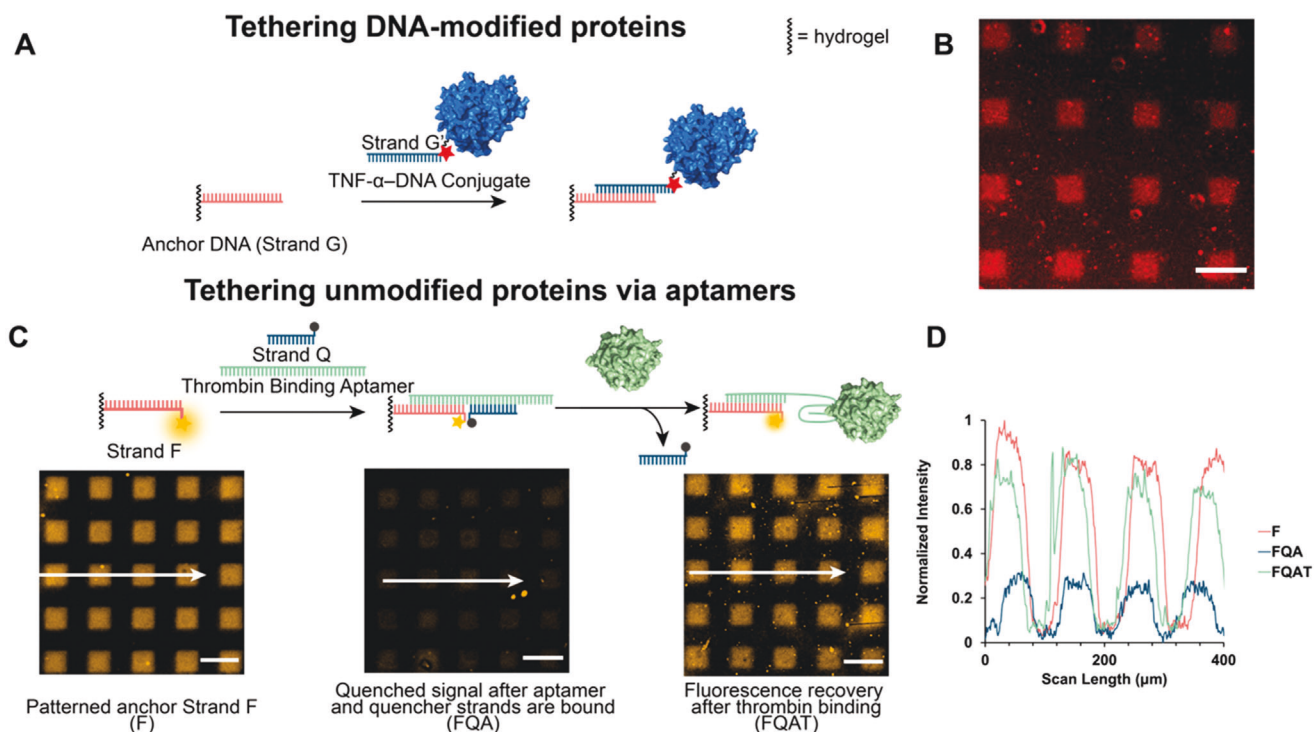
ADVANCED
SCIENCE NEWS
www.advancedsciencenews.com

ADVANCED
MATERIALS
www.advmat.de

Figure 4. A) Tethering DNA-modified proteins is achieved by first patterning complementary sequence in hydrogels and allowing protein–DNA conjugate to diffuse through the network and bind to the DNA patterns. B) Confocal micrograph of TNFα in patterns. C) Tethering unmodified proteins is achieved via aptamer–protein interactions. Images shown are confocal micrographs. First, Strand F is patterned to in the gel (Left). Next, the gels are swollen in a solution of 10 μm Strand Q and 10 μm thrombin binding aptamer (TBA) and washed (Middle). Last, a 1 μm solution of thrombin is introduced. D) Normalized profile plots of confocal micrographs show fluorescence quenching when Strand Q and TBA are introduced. Data are normalized to maximum fluorescence values of the "F" gel. Fluorescence recovery is observed after thrombin addition. Scale bars = 100 μm.

thermodynamically favorable. To monitor this strand displacement reaction, thiazole orange (TO) was attached as a surrogate nucleobase to the middle of Strand E.[45] This visco-sensitive dye fluoresces only upon forced intercalation in the oligonucleotide duplex and rotation around its methine bridge is restricted. We observed fluorescence turn on in patterned regions, indicating Strand E was hybridized to Strand D (Figure 3B). After Strand E′ was introduced to the system and the hydrogels were washed, the fluorescence was turned off, suggesting successful strand displacement. In addition, we observed that fluorescence in patterned areas could be recovered when reintroducing Strand E to the system, suggesting that this displacement reaction is repeatable. These results demonstrate that DNA sequence design can provide modular control over which strands can be bound and released within patterned domains. Further, use of oligonucleotides as stimuli for controlled release is advantageous in cell culture over cytotoxic chemical and stimuli (i.e., pH, temperature, or UV light), without sacrificing spatial control.

2.3. Directing Protein Attachment With Patterned DNA

Spatially-encoding proteins within hydrogels provides a platform for studying how the amount, arrangement, and release kinetics of cell-signaling protein regulate cellular pathways. To assess the ability of patterned oligonucleotides to direct the localization of proteins within hydrogels, we explored two routes: 1) modifying

proteins with DNA and using DNA–DNA interactions to direct protein location, and 2) using aptamer–protein interactions to direct the binding of unmodified proteins. Tumor necrosis factor alpha (TNFα), which is a secreted proinflammatory cytokine, was chosen as a model protein for the first approach. Patterning TNFα in hydrogels can provide insight on its role as a cytokine in regulating of immune cells as a T-cell effector and organogenesis. To synthesize the protein–DNA conjugates, TNFα was reacted with four equivalents of a PEG linker containing an *n*-hydroxysuccinimide (NHS) activated ester group and an azide.[46] After lysine conjugation to install the azide on the surface of TNFα, DNA containing a dibenzocyclooctyne (DBCO) (Strand G′ in **Figure 4**) was added to the reaction to attach DNA to TNFα via a strain-promoted azide–alkyne cycloaddition reaction. The conjugates were purified from the free DNA using size exclusion chromatography and characterized with polyacrylamide gel electrophoresis, confirming that there was at least a single DNA strand attached to each TNAα (Figure S4, Supporting Information).

To pattern the TNFα-DNA conjugates, an anchor DNA Strand G was patterned in the hydrogel. An indirect patterned approach was used instead of direct covalent attachment of the protein–DNA conjugate to the gel because it introduced a method to dynamically trigger the release of the protein from the hydrogel through a strand displacement reaction. This design enables the study of activity of biochemical cues in both bound and unbound forms of the protein within the hydrogel matrix as a protein's
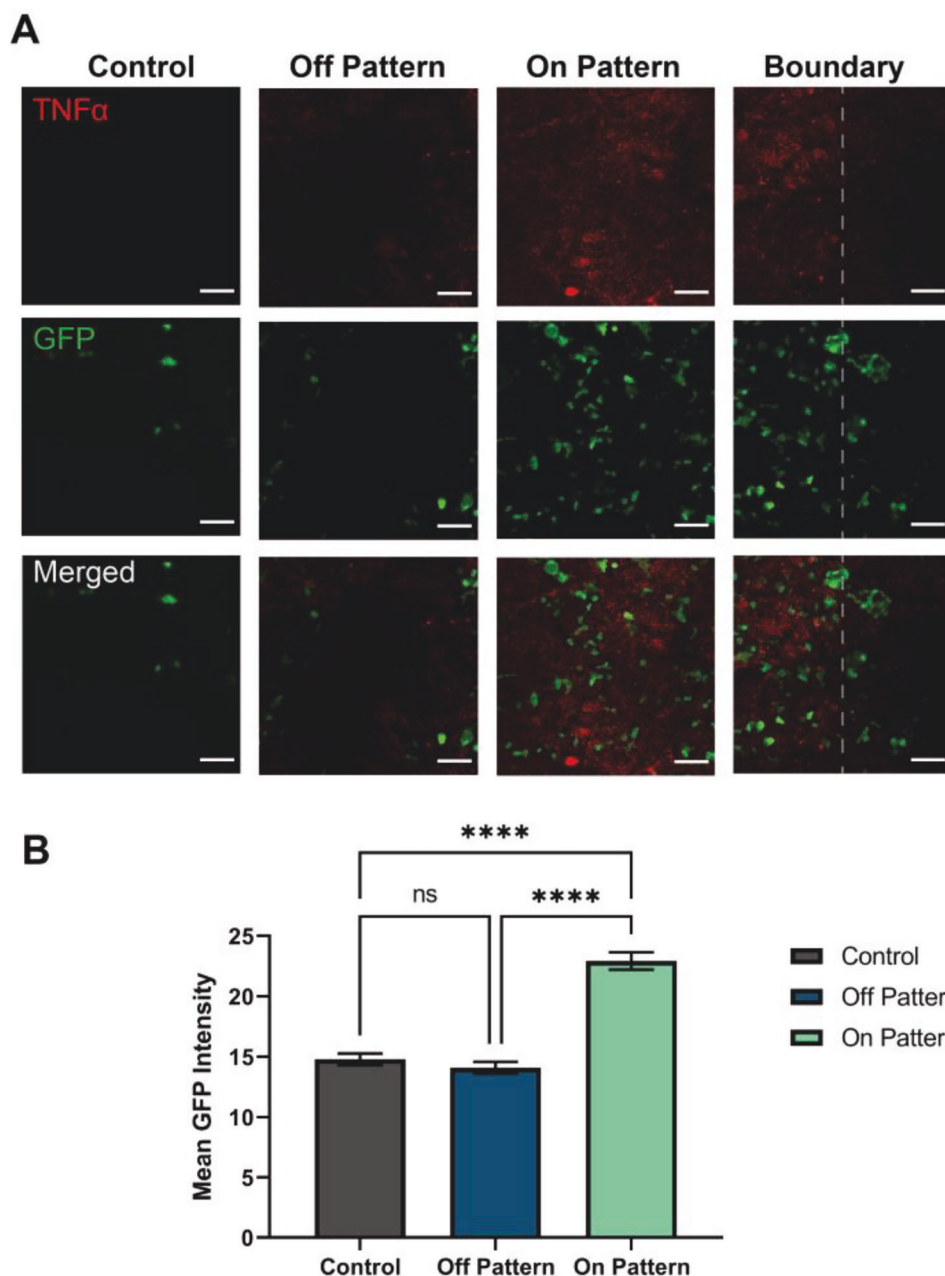
Figure 5. A) Confocal micrographs of GFP-HEK293 cells on varying regions of gels patterned with TNFα (off pattern, on pattern, and boundary) and control blank gels. B) Quantified mean GFP intensity from confocal micrographs of cells on control gels, outside of patterned area of gels, and on patterned area of gels. The results are presented as the mean $\pm$ SEM ($n = 250$). The statistical significance was analyzed using one-way ANOVA with Tukey's post-hoc test. **** indicates $p < 0.0001$, ns indicates $p > 0.05$.

bioactivity can vary between its soluble and tethered state.[47,48] After removing excess Strand G, a 5 μM solution of TNFα-DNA conjugate in 1$\times$ PBS was incubated with the hydrogel for 4 h. Excess conjugate was washed away with 1$\times$ PBS overnight and the gels were imaged with confocal microscopy. Confocal micrographs show that the TNFα-DNA conjugate was localized to the patterned areas of the gel, with minimal nonspecific adsorption or entrapment in the hydrogel. This model system demonstrates that oligonucleotide chemistry can be generalized for di-

recting protein–DNA conjugate attachment within hydrogels. These properties are important to replicate in synthetic hydrogels because in the ECM, cell signaling molecules (e.g., TNFα, VEGF, FGF, and TGFβ1) are sequestered and released on demand to activate signaling cascades.[49]

In some cases, proteins are highly sensitive to chemical modifications, which can lead to protein misfolding and loss of activity. To address this challenge, we used aptamer DNA strands, which are DNA sequences designed to bind selectively to analytes of

interest, including proteins. The model aptamer, thrombin binding aptamer (TBA), was selected due to its well characterized binding to the serine protease thrombin. To detect thrombin binding in the hydrogel, a three DNA strand construct was used.[50] First, a Cy3 fluorophore labeled sequence was patterned in the hydrogel (Strand F). Next, a sequence containing the 15 nt TBA, a region complementary to Strand F, and a region complementary to a Black Hole Quencher 2 (BHQ2) labeled third strand (Strand Q), was introduced. Upon hybridization of Strand Q and Strand F to the aptamer sequence, the fluorophore and quencher molecules were brought within the Förster radius, where BHQ2 could effectively quench the fluorescence of Cy3. In addition, Strand Q was designed to contain a 6 base overlap with the TBA to partially block the aptamer region of the sequence. Upon introduction of thrombin and folding of the aptamer, the quencher strand was displaced and an ≈threefold fluorescence recovery was observed. This approach enables the binding of proteins to hydrogels and a method for quantifying binding, which is useful in cases where DNA modification of proteins is challenging or leads to significant loss of activity.

2.4. Cellular Response to Patterned Chemical Factors

Directing cellular behavior using hydrogel scaffolds is critical for tissue engineering applications[18,19] and stem cell culture maintenance.[51] However, previous studies of cell behavior in DNA-functionalized hydrogels have been limited to gels functionalized with aptamer DNA throughout the hydrogel bulk. Therefore, we investigated whether our system could be used to pattern biochemical signals to affect cellular functions. To facilitate cell adhesion to the PEG hydrogel matrix, a peptide containing an arginine–glycine–aspartic acid (RGD) motif, terminated with an acrylate group, was copolymerized with the hydrogel precursors. NIH 3T3 mouse fibroblasts were seeded on the hydrogels and showed attachment within 24 h of seeding (Figure S16, Supporting Information). Cell survival on the alkyne-modified hydrogels was assessed by cell viability fluorescence assays. These assays revealed that the cells maintain their viability on the gels for at least a week (Figure S17, Supporting Information).

To study cellular response to patterned chemical cues, an engineered GFP-reporter HEK293 (GFP-HEK293) cell line was utilized to monitor activation of the nuclear factor Kappa B (NF-κB). In the presence of a ligand that can activate the NF-κB pathway (e.g., TNFα, IL-1β, and IL-17), the GFP-HEK293 cells express GFP in a concentration dependent manner, providing a fluorescence readout. Here, NF-κB activation was studied with TNFα as the signaling protein through patterning of TNFα-DNA conjugates in hydrogels. To ensure that cell activation for the TNFα-DNA conjugate did not differ from native TNFα, GFP expression was assessed for the GFP-HEK293 seeded in 12-well plates (Figure S18, Supporting Information) treated with varying concentrations of TNFα, TNFα-DNA conjugate, and DNA. 24 h after treatment, GFP expression was observed in a dose-dependent manner. This experiment confirmed that TNFα activity is maintained post-functionalization with DNA.

Next, GFP-HEK293 cell activation was studied on TNFα-bound hydrogels. RGD containing hydrogels, patterned with Strand G

uniformly over half of the gel, were swollen in a 2.5 µM solution of TNFα-DNA conjugate in cell media. GFP-HEK293 cells were seeded on the hydrogels and allowed to grow for 16 h to form a monolayer. GFP expression of cells on the pattern, outside of the pattern, and at the boundary was imaged via live cell confocal microscopy. Cells on gel regions containing TNFα showed an ≈twofold higher GFP expression compared to cells outside of the patterned areas (**Figure 5**), as evidenced by colocalization of the GFP signal and the Cy5 signal from TNFα-DNA conjugates. Notably, this difference is observable in the cells at the boundary of the patterned area, demonstrating that the cells confined to the pattern show greater activation. We also observed that cells at the pattern boundary or within 200 µm of the boundary express GFP at higher rates than cells at further distances from TNFα. These results indicate that spatial organization of protein signals within a hydrogel matrix can lead to different phenotypic outcomes for cells.

3. Conclusion

Here, we have established a chemistry for photopatterning DNA in hydrogels with high spatial resolution, where DNA hybridization can be reversibly controlled and DNA can direct protein attachment. This new strategy for patterning DNA in hydrogels will enable the study of complex signaling environments on cells, where highly multiplexed materials with orthogonal interactions can be generated by patterning multiple DNA sequences. This work and these techniques open up new avenues for studying fundamental cell–material interactions, including the role of multiple signals in cell signaling pathways, cell-to-cell communication between cells on differing patterns, and cell fate analysis of single cells.

4. Experimental Section

Hydrogel Synthesis: Hydrogel thin films were formed on acrylated substrates for ease of patterning. Glass microscope slides were cleaned, treated with O$_2$ plasma, and added to a desiccator with an open vial of 5 mL of 20% v/v of 3-(trimethoxysilyl)propyl acrylate (Sigma–Aldrich, 475149) in toluene. The substrates were left for 24 h to allow for acrylate monolayer formation. A hydrogel precursor solution consisting of 2.5 wt% PEGDA (MW = 3400 Da), 7.5 wt% methoxy poly(ethylene glycol) monoacrylate (PEGMA, MW = 480 Da, Sigma–Aldrich, 454 990), and 1 wt% propargyl acrylate (PA, MW = 110.11 Da) was prepared in 20% MeOH/water. To initiate free radical polymerization, 2 µL of 0.2 M ammonium persulfate (APS) and 1 µL of 0.1 M tetramethylethylenediamine (TEMED) were added to 77 µL of precursor solution. The 80 µL solution was quickly mixed and pipetted into a mold formed by the acrylated glass slide, a 0.5 mm silicon spacer, and a glass coverslip. The reaction was left to proceed for an hour at room temperature, after which the coverslip and spacer were removed, and the gel was placed in water overnight to achieve their equilibrium swelling volume. The hydrogel was characterized via Fourier-transform infrared spectroscopy (FTIR) and via time-sweep rheology.

Hydrogel Photopatterning: Gels swollen with DNA were patterned with a Tera-FAB E-series instrument. First, the light projection from the DMD (coupled to a 5× or 20× microscope objective) was optically aligned to the surface of the gel using a 532 nm light source. Gels were then irradiated with a 405 nm light source with varying geometric feature sizes, light intensities, and exposure times. To remove unreacted DNA after patterning,

**ADVANCED
SCIENCE NEWS**

www.advancedsciencenews.com

**ADVANCED
MATERIALS**

www.advmat.de

gels were soaked in 2 mL of 1× PBS overnight and rinsed an additional three times with 2 mL of 1× PBS for 10 min.

DNA Loading Characterization: To determine average DNA concentration in hydrogels patterned with Cy3.5-labeled Strand A, gels ($n = 3$) were incubated in a 0.1 M NaOH solution, allowing for the base hydrolysis of esters and degradation of crosslinks. After 48 h, the gels were fully degraded. The solution was then lyophilized, reconstituted in a small volume of water, and transferred to a 96-well microwell plate. The fluorescence intensity of Cy3.5 (Ex./Em. = 580 nm/605 nm) was quantified on a BioTek Cytation 5 plate reader. A standard curve of known concentrations of Cy3.5-labeled Strand A was used to determine DNA concentration from fluorescence readings. The signal from blank hydrogels was subtracted from the measurements, and the values were normalized per area to give DNA loading per patterned area.

TNFα-DNA Conjugate Synthesis and Characterization: To synthesize TNFα-DNA conjugates, the protein was mixed with a heterobifunctional linker containing a N-hydroxysuccinimide group that could react with surface-exposed lysine residues of TNFα and an azide group for DNA attachment. First, a 50 μM solution of Human TNFα (Genscript, Z01001) in 1× phosphate buffered saline (PBS) was reacted with four equivalents of Azido-PEG$_{12}$-NHS Ester (Quanta Biodesign, 10505) for 1 h at room temperature. The reaction mixture was run through a NAP-10 desalting column (Cytiva, 17-0854-02) equilibrated in 1× PBS to remove excess linker. Next, eight equivalents of DBCO-terminated DNA (Strand G' [TNFα-DNA Linker]) were added to the TNFα-N$_3$ solution and the strain promoted azide–alkyne cycloaddition was allowed to proceed for 16 h at room temperature. The TNFα-DNA conjugate was concentrated with a 10K MWCO spin filter by centrifugation at $5000 \times g$ for 15 min. To separate the protein–DNA conjugate from free DNA, the sample was purified on a Bio-Rad ENrich SEC 650 preparatory column on a Bio-Rad NGC Quest 10 Plus Chromatography System, with 1× PBS as an elution buffer and a flow rate of 0.5 mL min^{-1}. Samples were characterized using analytical sodium dodecyl sulfate polyacrylamide gel electrophoresis (SDS-PAGE) and UV–vis spectroscopy.

Cell Viability Assay: To test if the hydrogels containing PA have any cytotoxic effects, a cellular viability assay was performed. NIH 3T3 mouse fibroblasts were seeded (100,000 cells per gel) on gels containing 1 wt% PA and 15 mM GRGDSG peptide and monitored over the course of a week. A live/dead cell imaging kit (Invitrogen, R37601) was used containing a live cell permeable stain calcein AM (green channel) and a nonpermeable dead cell stain (red channel). Gel replicates were stained and imaged 1, 4, and 7 days after cell seeding. On day 7, ≈95% of cells on the hydrogels remained alive, indicating cells maintain their viability on these hydrogels.

HEK293-GFP Cell Seeding and Assay: RGD peptide containing hydrogels was patterned with Strand G, such that half of the gel area was functionalized with DNA. Next, the gels were soaked in a 1 mL solution of 1 μM TNFα-Strand G' conjugate in 1× PBS to allow hybridization of Strand G' to Strand G. Unbound TNFα-Strand G' conjugate was washed five times with 2 mL of 1× PBS over the course of 2 days. After fluorescence optical imaging to confirm pattern formation, the gels were transferred to chambered coverslips for cell seeding (ibidi USA, Inc., 80 427). HEK293-GFP cells (Systems Biosciences, TR860A-1), which report NF-κB signaling, were seeded on the gels at a concentration of 250,000 cells per hydrogel. To maximize cell attachment to the gels, the cells were suspended in 50 μL of DMEM, added to the top of the gels, and placed in a cell incubator for 1 h. Next, 1 mL of DMEM was added to each well. 16 h after cell seeding, the cells were imaged via confocal microscopy to measure GFP expression.

Confocal Microscopy and Image Analysis: Confocal microscopy was performed using a Zeiss Laser Scanning Microscope (Zeiss LSM800). Images were acquired for each experiment using identical parameters for each sample (e.g., laser power, master gain, pinhole size, scan speed, and offset), and analyzed identically using ImageJ. To determine pattern resolution, confocal micrographs were taken at various regions of each hydrogel, and multiple line scans were taken across images to quantify fluorescence intensity. The average full width at half maximum (FWHM) of the peaks was calculated from the line profiles (reported as mean ± standard deviation, $n = 50$ features). To quantify cell activation of HEK293-GFP cells, mean GFP intensity was determined for cells on control gels, outside of patterned area of gels, and on patterned area of gels using ImageJ particle analysis. The results are presented as the mean ± SEM ($n = 250$). The statistical significance was analyzed using one-way ANOVA using GraphPad Prism.

Statistical Analysis: All data were analyzed and plotted using GraphPad Prism 9.0. Line profiles for Figure 4C were normalized to the maximum fluorescence value. For all data, sample sizes are indicated in the figure caption. The gels were analyzed with a sample size of $n = 3$. The results in Figure 5B were analyzed using a one-way ANOVA with Tukey's post-hoc test. The significance values are indicated with **** as $p < 0.0001$ and ns as $p > 0.05$.

Supporting Information

Supporting Information is available from the Wiley Online Library or from the author.

Conflict of Interest

C.A.M. has financial interests in TERA-print LLC which could potentially benefit from the outcomes of this research.

Data Availability Statement

The data that support the findings of this study are available from the corresponding author upon reasonable request.

[1] G. Weng, U. S. Bhalla, R. Iyengar, *Science* **1999**, *284*, 92.

[2] C. Frantz, K. M. Stewart, V. M. Weaver, *J. Cell Sci.* **2010**, *123*, 4195.

[3] R. O. Hynes, A. Naba, *Cold Spring Harbor Perspect. Biol.* **2012**, *4*, a004903.

[4] E. Oh, B. Meckes, J. Chang, D. Shin, C. A. Mirkin, *Adv. NanoBiomed. Res.* **2022**, *2*, 2100131.

[5] M. Lin, B. Meckes, C. Chen, M. H. Teplensky, C. A. Mirkin, *ACS Cent. Sci.* **2022**, *8*, 1282.

[6] L. R. Giam, M. D. Massich, L. L. Hao, L. S. Wong, C. C. Mader, C. A. Mirkin, *Proc. Natl. Acad. Sci. USA* **2012**, *109*, 4377.

[7] M. D. Cabezas, B. Meckes, C. A. Mirkin, M. Mrksich, *ACS Nano* **2019**, *13*, 11144.

[8] M. J. Dalby, N. Gadegaard, R. O. Oreffo, *Nat. Mater.* **2014**, *13*, 558.

[9] J. E. Leslie-Barbick, C. Shen, C. Chen, J. L. West, *Tissue Eng., Part A* **2011**, *17*, 221.

[10] X. Liu, R. Liu, B. Cao, K. Ye, S. Li, Y. Gu, Z. Pan, J. Ding, *Biomaterials* **2016**, *111*, 27.

[11] A. J. Engler, S. Sen, H. L. Sweeney, D. E. Discher, *Cell* **2006**, *126*, 677.

[12] R. D. Piner, J. Zhu, F. Xu, S. Hong, C. A. Mirkin, *Science* **1999**, *283*, 661.

[13] K. B. Lee, S. J. Park, C. A. Mirkin, J. C. Smith, M. Mrksich, *Science* **2002**, *295*, 1702.

[14] G. Liu, S. H. Petrosko, Z. Zheng, C. A. Mirkin, *Chem. Rev.* **2020**, *120*, 6009.

[15] J. A. Lewis, *Adv. Funct. Mater.* **2006**, *16*, 2193.

[16] S. M. Hull, L. G. Brunel, S. C. Heilshorn, *Adv. Mater.* **2022**, *34*, 2103691.

[17] A. Kumar, G. M. Whitesides, *Appl. Phys. Lett.* **1993**, *63*, 2002.

[18] C. A. DeForest, K. S. Anseth, *Annu. Rev. Chem. Biomol. Eng.* **2012**, *3*, 421.

[19] Y. S. Zhang, A. Khademhosseini, *Science* **2017**, *356*, eaaf3627.

[20] S. P. B. Teixeira, R. M. A. Domingues, M. Shevchuk, M. E. Gomes, N. A. Peppas, R. L. Reis, *Adv. Funct. Mater.* **2020**, *30*, 1909011.

[21] R. J. Wade, E. J. Bassin, W. M. Gramlich, J. A. Burdick, *Adv. Mater.* **2015**, *27*, 1356.

[22] S. P. Singh, M. P. Schwartz, J. Y. Lee, B. D. Fairbanks, K. S. Anseth, *Biomater. Sci.* **2014**, *2*, 1024.

[23] C. A. DeForest, B. D. Polizzotti, K. S. Anseth, *Nat. Mater.* **2009**, *8*, 659.

[24] C. Yang, F. W. DelRio, H. Ma, A. R. Killaars, L. P. Basta, K. A. Kyburz, K. S. Anseth, *Proc. Natl. Acad. Sci. USA* **2016**, *113*, E4439.

[25] J. C. Grim, T. E. Brown, B. A. Aguado, D. A. Chapnick, A. L. Viert, X. Liu, K. S. Anseth, *ACS Cent. Sci.* **2018**, *4*, 909.

[26] P. M. Gawade, J. A. Shadish, B. A. Badeau, C. A. DeForest, *Adv. Mater.* **2019**, *31*, 1902462.

[27] J. A. Shadish, G. M. Benuska, C. A. DeForest, *Nat. Mater.* **2019**, *18*, 1005.

[28] J. S. Kahn, Y. Hu, I. Willner, *Acc. Chem. Res.* **2017**, *50*, 680.

[29] Y. H. Wei, K. Z. Wang, S. H. Luo, F. Li, X. L. Zuo, C. H. Fan, Q. Li, *Small* **2022**, *18*, 2107640.

[30] O. J. Scheideler, C. Yang, M. Kozminsky, K. I. Mosher, R. Falcon-Banchs, E. C. Ciminelli, A. W. Bremer, S. A. Chern, D. V. Schaffer, L. L. Sohn, *Sci. Adv.* **2020**, *6*, eaay5696.

[31] A. Stejskalova, N. Oliva, F. J. England, B. D. Almquist, *Adv. Mater.* **2019**, *31*, 1806380.

[32] B. Soontornworajit, J. Zhou, M. T. Shaw, T. H. Fan, Y. Wang, *Chem. Commun.* **2010**, *46*, 1857.

[33] J. Lai, P. Jiang, E. R. Gaddes, N. Zhao, L. Abune, Y. Wang, *Chem. Mater.* **2017**, *29*, 5850.

[34] Z. Zhang, C. Liu, C. Yang, Y. Wu, F. Yu, Y. Chen, J. Du, *ACS Appl. Mater. Interfaces* **2018**, *10*, 8546.

[35] S. B. Ebrahimi, D. Samanta, H. F. Cheng, L. I. Nathan, C. A. Mirkin, *J. Am. Chem. Soc.* **2019**, *141*, 13744.

[36] D. Y. Zhang, G. Seelig, *Nat. Chem.* **2011**, *3*, 103.

[37] F. Huang, M. Chen, Z. Zhou, R. Duan, F. Xia, I. Willner, *Nat. Commun.* **2021**, *12*, 2364.

[38] A. Cangialosi, C. Yoon, J. Liu, Q. Huang, J. Guo, T. D. Nguyen, D. H. Gracias, R. Schulman, *Science* **2017**, *357*, 1126.

[39] J. A. Beamish, J. Zhu, K. Kottke-Marchant, R. E. Marchant, *J. Biomed. Mater. Res., Part A* **2010**, *92*, 441.

[40] A. B. Lowe, C. E. Hoyle, C. N. Bowman, *J. Mater. Chem.* **2010**, *20*, 4745.

[41] H. Y. Peng, C. Wang, W. X. Xi, B. A. Kowalski, T. Gong, X. L. Xie, W. T. Wang, D. P. Nair, R. R. McLeod, C. N. Bowman, *Chem. Mater.* **2014**, *26*, 6819.

[42] M. Mitmoen, O. Kedem, *ACS Appl. Mater. Interfaces* **2022**, *14*, 32696.

[43] A. Y. Sim, J. Lipfert, D. Herschlag, S. Doniach, *Phys. Rev. E* **2012**, *86*, 021901.

[44] B. D. Fairbanks, M. P. Schwartz, C. N. Bowman, K. S. Anseth, *Biomaterials* **2009**, *30*, 6702.

[45] F. Hovelmann, I. Gaspar, A. Ephrussi, O. Seitz, *J. Am. Chem. Soc.* **2013**, *135*, 19025.

[46] P. H. Winegar, C. A. Figg, M. H. Teplensky, N. Ramani, C. A. Mirkin, *Chem* **2022**, *8*, 3018.

[47] I. Batalov, K. R. Stevens, C. A. DeForest, *Proc. Natl. Acad. Sci. USA* **2021**, *118*, e2014194118.

[48] B. Varnum-Finney, L. Z. Wu, M. Yu, C. Brashem-Stein, S. Staats, D. Flowers, J. D. Griffin, I. D. Bernstein, *J. Cell Sci.* **2000**, *113*, 4313.

[49] A. M. Rosales, K. S. Anseth, *Nat. Rev. Mater.* **2016**, *1*, 15012.

[50] R. Nutiu, Y. Li, *J. Am. Chem. Soc.* **2003**, *125*, 4771.

[51] C. M. Madl, S. C. Heilshorn, *Annu. Rev. Biomed. Eng.* **2018**, *20*, 21.